# Relativistic breakdown in planetary atmospheres

J. R. Dwyer
*Department of Physics and Space Sciences, Florida Institute of Technology, Melbourne, Florida 32901*

(Received 30 November 2006; accepted 25 January 2007; published online 16 April 2007)

In 2003, a new electrical breakdown mechanism involving the production of runaway avalanches by positive feedback from runaway positrons and energetic photons was introduced. This mechanism, which shall be referred to as "relativistic feedback," allows runaway discharges in gases to become self-sustaining, dramatically increasing the flux of runaway electrons, the accompanying high-energy radiation, and resulting ionization. Using detailed Monte Carlo calculations, properties of relativistic feedback are investigated. It is found that once relativistic feedback fully commences, electrical breakdown will occur and the ambient electric field, extending over cubic kilometers, will be discharged in as little as $2\times10^{-5}$ s. Furthermore, it is found that the flux of energetic electrons and x rays generated by this mechanism can exceed the flux generated by the standard relativistic runaway electron model by a factor of $10^{13}$, making relativistic feedback a good candidate for explaining terrestrial gamma-ray flashes and other high-energy phenomena observed in the Earth's atmosphere. © *2007 American Institute of Physics*. [DOI: 10.1063/1.2709652]

## I. INTRODUCTION

Runaway electrons are ubiquitous in plasmas and gaseous media in which electric fields are present, occurring in conditions ranging from hot plasmas inside tokamaks[1–8] to thunderstorms in the upper and middle atmospheres, to lightning discharges at sea level.[9] Runaway electrons are produced when the electric force exceeds the effective drag force in the medium, caused predominantly by energy losses from ionization, bremsstrahlung emission, and (for tokamaks) synchrotron emission.[10–12] These electrons can gain large energies from the electric field, reaching many tens of MeV (Refs. 13–15). When runaway electrons collide with gas atoms or plasma ions, they emit bremsstrahlung radiation in the form of x rays with energies extending up into the multi-MeV range. Such x rays are frequently observed during tokamak disruptions[16,17] and have recently been observed from natural and rocket-triggered lightning near the ground[18–22] from thunderstorms,[23–25] from laboratory sparks in air,[26] and in outer space in the form of terrestrial gamma-ray flashes (TGFs).[27–29] In fully ionized laboratory plasmas, the observed high-energy x rays certainly come from runaway electrons, and to date, the only viable explanation for such x-ray/gamma-ray emission in air is from runaway electrons. However, up until recently, the large fluxes of x rays and gamma rays observed in the atmosphere have been difficult to explain using existing models of runaway electron production, and indeed the source mechanism(s) are still under active debate.[13]

Over the past decade, in light of the x-ray observations, runaway electrons have gained great popularity for explaining thunderstorm and lightning processes, especially the initiation of lightning.[30] How lightning is initiated in the relatively weak electric fields measured inside thunderstorms has remained one of the great mysteries in the atmospheric sciences.[31,32] A model introduced by Gurevich *et al.* in 1992, commonly referred to as the "relativistic runaway electron avalanche (RREA) model,"[33] has received much attention in recent years. In this model, an avalanche of relativistic runaway electrons is generated via hard elastic scattering of runaway electrons with atomic electrons in the gas. The threshold electric field for the production of runaway avalanches by this mechanism has been found to be $E_{th}=284$ kV/m for air at sea level,[34] a value comparable to electric field strengths commonly measured inside thunderstorms. Unfortunately, this mechanism has not yet been able to demonstrate how a large-scale, diffuse discharge can lead to the creation of a hot leader (plasma) channel and lightning.[35] Furthermore, in order to produce large enough fluxes of runaway electrons to create a partially ionized plasma that can significantly affect the electrical properties of the environment, very large avalanche regions must be presupposed, with exceedingly large potential differences.

These difficulties, to a great extent, were overcome by the introduction of a new gas breakdown mechanism by Dwyer[34] involving positive feedback effects from positrons and energetic photons.[36] In this mechanism, avalanches of runaway electrons emit bremsstrahlung x rays that may either Compton backscatter or pair produce in the gas medium. If the backscattered photons propagate to the start of the avalanche region and produce another runaway electron, either via Compton scattering or photoelectric absorption, then a secondary avalanche is created. Alternatively, the positrons created by pair production can sometimes turn around in the ambient electric field and run away in the opposite direction of the electrons. The positrons quickly become relativistic, allowing them to travel for many hundreds of meters before annihilating. If these positrons propagate to the start of the avalanche region they can produce additional runaway electrons via hard elastic scattering with atomic electrons in the gas (i.e., Bhahba scattering), thereby producing secondary avalanches. These secondary avalanches can in turn emit more x rays that Compton scatter or pair produce, resulting in more feedback and more avalanches. This positive feedback effect allows the runaway discharge to become self-

 

sustaining, no longer requiring an external source of energetic seed electrons. As a result of this positive feedback, the number of runaway electron avalanches increases exponentially on a time scale measured in microseconds.

The two principal feedback mechanisms, which shall be referred to as x-ray feedback (also called gamma-ray or photon feedback) and positron feedback, were originally described by Dwyer,[34] who also used a Monte Carlo simulation to calculate the electric field thresholds necessary for feedback to be important. In addition, second-order feedback effects can also occur such as feedback from bremsstrahlung x rays emitted from the backward propagating positrons and feedback from the 511-keV gamma rays emitted by the annihilating positrons. These feedback mechanisms shall be referred to as positron bremsstrahlung feedback and positron annihilation feedback, respectively. As will be discussed below, these second-order effects generally occur at rates at or below about 10% that of the positron and x-ray feedback. To distinguish the feedback mechanisms described here, which involve high-energy particles, from the low-energy feedback mechanisms occurring in ordinary Townsend gas discharges, in this paper, the four feedback mechanisms above shall jointly be referred to as "relativistic feedback" (RF).

As will be discussed below in Sec. IV, the effects of relativistic feedback can increase the flux of runaway electrons and the accompanying x-ray emission by factors of trillions, resulting in a partially ionized plasma and a large increase in the conductivity that ultimately collapses the ambient electric field under conditions for which an ordinary runaway discharge has a completely negligible effect. Indeed, Dwyer[34] showed that this mechanism establishes an upper limit on the large-scale static electric field that is achievable in air, even in principle. If this limit is exceeded, even by a small amount, then the flux of runaway electrons increases exponentially to the point where the electric field is quickly reduced below the limit.

In this paper, a detailed investigation of the relativistic feedback mechanisms is presented for both air and the hydrogen–helium atmospheres of the four Jovian planets, expanding upon earlier work by Dwyer *et al.*[34,37,38] and Babich *et al.*[36] It will be shown that relativistic feedback leads to a new kind of electrical breakdown in gaseous media and, therefore, is a new mechanism for generating plasmas in such media. Unlike the RREA mechanism, which is often and erroneously called "runaway breakdown," this new type of electrical breakdown produced by relativistic feedback is a true breakdown under the standard use of the term.

## II. MONTE CARLO SIMULATION

### A. Relativistic runaway electron avalanche overview

The basic mechanism for producing runaway electrons is illustrated in Fig. 1, which shows the effective drag force due to collisions of electrons with air as a function of the electron's kinetic energy.[13] For kinetic energies $K > K_{\mathrm{th}}$, the rate of energy gain from the electric field, $eE$, exceeds the rate of energy loss due to collisions, making it possible for electrons to acquire large amounts of energy. For very large electric fields, $E > E_c$, the high-energy tail of the bulk free electron population can run away.[39,40] At lower electric fields, $E_{\mathrm{th}} < E < E_c$, the initial runaway electrons must be supplied by external energetic "seed" particles. However, as the electrons propagate they occasionally collide with air atoms producing energetic "knock-on" electrons, which in turn can run away. The result is an avalanche of relativistic electrons that increases in size exponentially with distance. Note that the effective drag force shown in Fig. 1 depends linearly on the air density. Therefore, the electric field necessary for electrons to run away also depends linearly on the density and so is lower at high altitudes.[41]

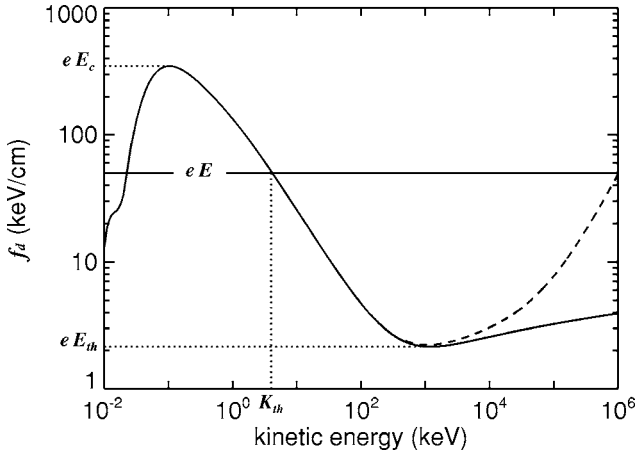


FIG. 1. The effective drag force experienced by a free electron moving through air at STP as a function of kinetic energy (Ref. 13). The solid curve is due to inelastic scattering of the electron with air molecules, and the dashed curve includes the effects of bremsstrahlung emission. The horizontal line shows the electric force from a 500-kV/m electric field. Runaway electrons occur for kinetic energies greater than the threshold energy, $K > K_{\mathrm{th}}$. $E_c$ is the critical electric field strength for which low-energy thermal electrons will run away, and $E_{\mathrm{th}}$ is the minimum field needed to produce relativistic runaway electrons.

### B. Monte Carlo overview

The Monte Carlo simulation of relativistic runaway electron avalanches used in this study is capable of modeling the development and propagation of runaway electron avalanches in any gaseous medium for both spatially and time-varying electric and magnetic fields.[13,29,34,37,38,42] This simulation includes, in an accurate form, all the important interactions involving runaway electrons, positrons, x rays, and gamma rays. These interactions include energy losses through ionization and atomic excitation, and Møller scattering.[43] The simulation fully models elastic scattering using a shielded-Coulomb potential and includes bremsstrahlung production of x rays and gamma rays, and the subsequent propagation of the photons, including photoelectric absorption, Rayleigh scattering, Compton scattering, and pair production. In addition, the simulation includes positron propagation (and annihilation) and the generation of energetic seed electrons via Bhabha scattering of positrons, and via Compton scattering and photoelectric absorption of energetic photons.

### C. Detailed physics used in the Monte Carlo

For electrons with kinetic energies above a few hundred eV, ionization/atomic excitation energy losses per unit length are well described by the Bethe equation,[43]

$$f_d = \frac{2\pi NZr_e^2 mc^2}{\beta^2} \times \left[ \ln\left( \frac{m^2c^4(\gamma^2-1)(\gamma-1)}{I^2} \right) - \left(1 + \frac{2}{\gamma} - \frac{1}{\gamma^2}\right)\ln 2 + \frac{1}{\gamma^2} + \frac{(\gamma-1)^2}{8\gamma^2} - \delta(\gamma) \right], \quad (1)$$

where $N$ is the number density of the gas atoms and $Z$ is the average atomic number of the gas atoms; $r_e$ is the classical electron radius, $mc^2$ is the rest mass energy of an electron, $\beta = v/c$ and $\gamma$ is the Lorentz factor of the energetic electron, $I$ is the effective ionization potential (e.g., $I = 85.7$ eV for air), and $\delta$ is a correction due to the density effect. For air, the density effect correction is very small below 30 MeV and increases only slowly above that energy.

The energy loss rate described by Eq. (1) produces an effective drag force acting on the particle, also called the dynamical friction, with the magnitude given by Eq. (1) and the direction opposite the particle's velocity vector.

For a given electric field strength, the runaway threshold kinetic energy, $K_{\text{th}}$, is evaluated by setting the magnitude of the electric force equal to the effective drag force given by Eq. (1) and solving numerically for $\gamma$. Simulations have shown that it is extremely unlikely for an electron emitted in any direction to run away for energies at or below this value. For varying electric fields, $K_{\text{th}}$ is calculated locally for each position and time.

Møller scattering (electron-electron elastic scattering) of the runaway electrons with atomic (or free) electrons is fully modeled by the Monte Carlo simulation for electron kinetic energies above a specified threshold (usually $K_{\text{th}}$). The Møller scattering cross section is given by[43]

$$\frac{d\sigma_{\text{Møller}}}{dK} = \frac{2\pi r_e^2 mc^2}{\beta^2}\left[ \frac{(\gamma-1)^2 m^2c^4}{K^2(mc^2(\gamma-1)-K)^2} - \frac{(2\gamma^2+2\gamma-1)}{K(mc^2(\gamma-1)-K)\gamma^2} + \frac{1}{m^2c^4\gamma^2} \right], \quad (2)$$

where $K$ is the kinetic energy of the scattered atomic electron.

Because the energy losses from Møller scattering are directly modeled in the simulation, these losses should not also be included in the ionization energy loss $f_d$. This is remedied by subtracting off the quantity

$$f_{\text{Møller}} = NZ\int_{K_{\text{th}}}^{mc^2(\gamma-1)/2} K\frac{d\sigma_{\text{Møller}}}{dK}dK = \frac{2\pi NZr_e^2 mc^2}{\beta^2}\left[ \ln\left( \frac{mc^2(\gamma-1)}{2K_{\text{th}}} \right) + 1 - \frac{K_{\text{th}}}{(mc^2(\gamma-1)-K_{\text{th}})} - \left(1 + \frac{2}{\gamma} - \frac{1}{\gamma^2}\right)\ln\left( \frac{2(mc^2(\gamma-1)-K_{\text{th}})}{mc^2(\gamma-1)} \right) + \frac{(\gamma-1)^2}{8\gamma^2} - \frac{K_{\text{th}}^2}{2m^2c^4\gamma^2} \right], \quad (3)$$

from Eq. (1) when calculating the effective drag force.[41]

The secondary electrons produced by Møller scattering can themselves be energetic enough to run away and are therefore added to the simulation. In this way, the number of runaway electrons increases exponentially with distance for electric field strengths above the runaway avalanche threshold, $E_{\text{th}}$. In addition, similar ionization rate calculations are done for positrons, but the Møller scattering equation is replaced with the Bhabha scattering equation[43] and the effective drag force equation is modified accordingly.

Unlike electrons, when describing the propagation of positrons through a gas, positron annihilation must be included. The total cross section for two-photon annihilation of a positron with Lorentz factor, $\gamma$, with a stationary electron, is[43]

$$\sigma_{\text{annih}} = \frac{\pi r_e^2}{\gamma+1}\left[ \frac{(\gamma^2+4\gamma+1)}{(\gamma^2-1)}\ln(\gamma+\sqrt{\gamma^2-1}) - \frac{\gamma+3}{\sqrt{\gamma^2-1}} \right]. \quad (4)$$

Simulations show that many positrons are created with kinetic energies above 1 MeV. Even if created in a direction opposite their runaway direction, these positrons can quickly turn around and gain energy. As a result, many positrons reach energies in which their path length through air before annihilation is over 500 m at sea level, allowing a significant fraction to traverse the entire avalanche region (in the opposite direction of the electrons). When the positrons do annihilate, the two 511-keV gamma rays are then propagated by the simulation and allowed to interact. These 511-keV gamma rays can also produce energetic electrons that run away via Compton scattering or by photoelectric absorption after they Compton scatter down in energy.

As electrons and positrons propagate in a gaseous medium they experience elastic scattering with the atomic nuclei as well as the atomic electrons. Elastic scattering with the nuclei has an important impact upon the development of the runaway avalanches, since it tends to scatter electrons off the electric field lines, requiring a larger electric force to counterbalance the effective drag force due to ionization. The result is a higher electric field threshold and longer avalanche lengths for runaway avalanche development than would occur if elastic scattering were not present.

This elastic scattering is fully modeled using a shielded-Coulomb scattering cross section, which takes into account the charge distribution of both the nucleus and the atomic electrons in an atom.[44] This is calculated by multiplying the cross section for elastic scattering of the electron with the bare, point-like nucleus with the square modulus of the atomic form factor (i.e., the structure function), $F$,

$$\frac{d\sigma_{\mathrm{Coul}}}{d\Omega} = |F(q)|^2 \left(\frac{d\sigma_{\mathrm{Coul}}}{d\Omega}\right)_{\mathrm{nucleus}}, \tag{5}$$

where

$$\left(\frac{d\sigma_{\mathrm{Coul}}}{d\Omega}\right)_{\mathrm{nucleus}} = \frac{1}{4}\left(\frac{Zr_e}{\beta^2\gamma}\right)^2 \frac{(1-\beta^2\sin^2(\theta/2))}{\sin^4(\theta/2)}, \tag{6}$$

and

$$F(q) = -\frac{1}{Ze}\int \rho(r)\exp(-i\vec{q}\cdot\vec{x}/\hbar)d^3\vec{x}. \tag{7}$$

Here, $|\vec{q}|^2 = 4p^2\sin^2(\theta/2)$ is the momentum change of the electron during the collision and $\rho$ is the charge density for both the nucleus and the atomic electrons. Using the Thomas-Fermi model of the atom, the charge density is found to be

$$\rho(r) = Ze\,\delta^{(3)}(\vec{x}) - \frac{Ze}{4\pi a^2 r}\exp(-r/a), \tag{8}$$

with $a = 183.8\lambda\!\!\!^{-}Z^{-1/3}$, where $\lambda\!\!\!^{-}$ is the Compton wavelength.[45] This charge density produces the shielded-Coulomb potential,

$$V(r) = \frac{Ze}{4\pi\varepsilon_o r}\exp(-r/a). \tag{9}$$

Plugging Eq. (8) into the integral in Eq. (7) gives the form factor

$$F(q) = \frac{q^2}{q^2 + \hbar^2/a^2}. \tag{10}$$

The resulting shielded-Coulomb cross section for the elastic scattering of electrons is

$$\frac{d\sigma_{\mathrm{Coul}}}{d\Omega} = \frac{1}{4}\left(\frac{Zr_e}{\beta^2\gamma}\right)^2 \frac{(1-\beta^2\sin^2(\theta/2))}{\left(\sin^2(\theta/2) + \dfrac{\hbar^2}{4p^2a^2}\right)^2}. \tag{11}$$

Note that Eq. (11) applies for both electrons and positrons. It is relativistically correct and includes the effects of the particle's spin.

As electrons and positrons propagate through the medium they emit x rays via bremsstrahlung. While many approximate expressions exist for the bremsstrahlung cross section, the bremsstrahlung process relevant to runaway electrons and positrons involves a wide range of energies for both the incident electrons (positrons) and the emitted x rays. As a result, there is no single, simple formula that can accurately describe the emission, since the range covers nonrelativistic through ultrarelativistic energies with screening from the atomic electrons being important in some cases and not others. In order to calculate the bremsstrahlung cross section, a relativistically correct form must be used that incorporates the atomic form factor [Eq. (10)], similar to the calculation for the shielded-Coulomb scattering calculation. [Note that the best value to use for the constant $a$ appearing in Eqs. (8)–(10) can vary slightly for different scattering processes. For bremsstrahlung, the value $a = 111\lambda\!\!\!^{-}Z^{-1/3}$ was chosen so as to be consistent with earlier work.[46]] The resulting bremsstrahlung cross section is

$$d\sigma_{\mathrm{brem}} = \frac{Z^2 r_e^2 p_f dE_k d\Omega_k d\Omega_p}{4\pi^2 137 E_k p_o}\frac{m^2c^2}{q^4}|F(q)|^2\left\{\frac{p_f^2\sin^2\theta_f(4E_o^2 - q^2c^2)}{(E_f - p_f c\cos\theta_f)^2} + \frac{p_o^2\sin^2\theta_o(4E_f^2 - q^2c^2)}{(E_o - p_o c\cos\theta_o)^2}\right.$$
$$\left. - \frac{2p_f p_o\sin\theta_f\sin\theta_o\cos\phi(4E_fE_o - q^2c^2)}{(E_f - p_f c\cos\theta_f)(E_o - p_o c\cos\theta_o)} + \frac{2E_k^2(p_f^2\sin^2\theta_f + p_o^2\sin^2\theta_o - 2p_f p_o\sin\theta_f\sin\theta_o\cos\phi)}{(E_f - p_f c\cos\theta_f)(E_o - p_o c\cos\theta_o)}\right\}, \tag{12}$$

where[46]

$$q^2 = p_f^2 + p_o^2 + \frac{E_k^2}{c^2} - 2p_o\frac{E_k}{c}\cos\theta_o + 2p_f\frac{E_k}{c}\cos\theta_f$$
$$- 2p_f p_o(\cos\theta_f\cos\theta_o + \sin\theta_f\sin\theta_o\cos\phi).$$

In Eq. (12), $E_k$ is the energy of the emitted photon, $p_o$ and $p_f$ are the initial and final momenta of the electron, $E_o$ and $E_f$ are the initial and final total energies of the electron, $\theta_o$ and $\theta_f$ are the angles of the electron's momentum vectors with respect to the photon momentum vector $\vec{k}$, and $\phi$ is the angle between the planes $(\vec{p}_o,\vec{k})$ and $(\vec{p},\vec{k})$. The Monte Carlo evaluates Eq. (12) numerically to emit bremsstrahlung photons with the correct angular distribution and energy spectra.

Once photons are emitted via bremsstrahlung, the photon propagation involves four principle interactions: photoelectric absorption, Compton scattering, pair production, and Rayleigh scattering. At high energies, Compton scattering is well described by the famous Klein-Nishina formula.[43] At intermediate energies, coherent scattering becomes important and tabulated values are used. Tabulated values for the cross sections for photoelectric absorption and pair production are

also used.[47] Rayleigh scattering is calculated using the standard cross sections for this process.[48] In all cases, when secondary electrons or positrons are created from the basic interactions described above, their emission angle is calculated using the correct kinematics of the interaction and the new electrons and positrons are then added to the simulation.

### D. Monte Carlo applications

The general approach to simulating runaway avalanches is to emit some number of energetic seed electrons, simulating, for example, knock-on electrons from atmospheric cosmic rays into the start (bottom) of a high electric field region with $E > E_{\mathrm{th}}$. The runaway avalanches are then allowed to develop, and all particles, photons, electrons, and positrons above some energy (usually $K_{\mathrm{th}}$) are simulated. For a uniform field geometry, the number of particles is measured in planes perpendicular to the field lines. With such a technique the avalanche threshold in air, $E_{\mathrm{th}}$, at a number density, $n$, has been found to be $(284\ \mathrm{kV/m}) \times (n/n_o)$ for air, where $n_{\mathrm{o}} = 2.69 \times 10^{25}\ \mathrm{m}^{-3}$ is the number density of air molecules at standard conditions.[34,42] The avalanche (e-folding) length is well fit by the empirical relation,

$$\lambda = \frac{7300\ \mathrm{kV}}{(E - (276\ \mathrm{kV/m}) n/n_o)}, \tag{13}$$

valid over the range 300–2600 kV/m, where the electric field, $E$, is measured in kV/m (Refs. 34 and 42).

### E. Runaway electron sampling

Unlike the case of air, in hydrogen-helium atmospheres the runaway avalanches that produce significant amounts of feedback are too large to make the simulation of every runaway electron practical (see Fig. 14 below). For this reason, for the calculations for hydrogen-helium presented below, only a sample of the runaway electrons is fully simulated, and these electrons carry a weighting factor to represent the actual number of runaway electrons. Because the runaway electron energy distribution rapidly becomes self-similar, it is not necessary to fully simulate every runaway electron in order to capture the accurate physics of the avalanche. However, the feedback processes are relatively rare compared with the number of runaway electrons and so it is important to fully simulate the processes leading to feedback. This is mainly accomplished by randomly removing the secondary electrons created by Møller scattering with a probability, $p$. The secondary electrons that are not removed are then given a weighting factor of $1/(1-p)$ times the weighting factor that the parent electron (that created the secondary electrons) already possessed.

In order to simulate the feedback processes, bremsstrahlung emission is fully modeled according to the weighting factors of the electrons. For example, a runaway electron carrying a weight of 100, i.e., it represents 100 electrons in the simulation, is allowed to go through the bremsstrahlung process 100 times. (The energy of the electron is only allowed to change during the last process.) Any secondary electrons or positrons resulting from the bremsstrahlung x rays are then created with a starting weight of 1. For each electric field value, simulations are typically done with approximately 10 000 electrons at a time, and simulations are repeated, typically 10–200 times, until the required statistical precision is obtained.

In order to study the role of positron and x-ray feedback in runaway breakdown, the simulations for this work used a uniform electric field, with magnitude greater than the runaway threshold, directed down along the axis of a cylindrical volume of length $L$ and radius $R$, with $R \gg L$ unless otherwise specified. Outside the volume, the field is zero, and all particles continue to be propagated after they leave the volume until their energy is lost. Each simulation is initiated by injecting high-energy seed electrons into the bottom of the simulation volume, representing, for example, knock-on electrons produced by cosmic rays. The avalanche is then propagated until all the particles leave the volume and subsequently lose their energy, or until they pass through the midpoint of the simulation volume as (second generation or higher) feedback electrons.

### F. Measuring feedback

Relativistic feedback is recorded by keeping track of the electrons and photons that pass through the plane midway between the top and bottom of the avalanche region. The initial runaway electrons and photons are labeled as first generation particles. Any secondary electrons, photons, or positrons, regardless of the production mechanisms, carry the same generation number as the runaway electrons that led to the new particle's production. Once an electron passes through the midplane, moving in the direction opposite the electric field vector, its generation number is increased by 1. The feedback factor, $\gamma$, is defined to be the ratio of the number of runaway electrons with generation number $N+1$, passing through the midplane, divided by the number of runaway electrons with generation number $N$, passing through the midplane. The feedback factor is analogous to the second Townsend coefficient for low-energy discharges.[49]

If $\tau$ is the average time between successive generations of electrons passing through the midplane, then the flux of runaway electrons will increase exponentially with an e-folding time of $\tau' = \tau/\ln(\gamma)$ (see Sec. IV for more details). For the results presented here, second generation electrons (i.e., electrons produced by feedback) that enter the midplane are removed from the simulation. Otherwise, due to the self-sustaining nature of relativistic feedback, the simulation would continue to run indefinitely. However, it has been verified that continuing the simulation out to higher generations does not alter the results.

### G. Jovian atmospheres

The observation of planetary lightning on the four Jovian planets[50] led Dwyer *et al.*[38] to explore the properties of runaway avalanches in the hydrogen-helium atmospheres of the gas giants Jupiter, Saturn, Uranus, and Neptune. They found that by several measures runaway discharges are more efficient in the Jovian atmospheres than in the terrestrial atmosphere. For example, the Jovian runaway avalanche threshold is about a factor of 8 below the terrestrial value and is

about a factor of 10 below the conventional breakdown threshold when effects of hydrometeors are included. However, in their paper, Dwyer *et al.*[38] did not address the effects of the feedback mechanisms. In this paper, the properties of the feedback mechanisms will be explored for the Jovian atmospheres as well as for air, and the thresholds for feedback in the Jovian atmospheres will be presented for the first time.

The Jovian atmospheres are primarily hydrogen and helium with only trace amounts of other species. Dwyer *et al.*[38] showed that runaway avalanches are not sensitive to the exact abundance of helium. Specifically, the helium abundance made almost no difference for $He/H_2$ mole fractions between 0% and 20%, a range that encompasses the abundances in the four gas giants. In this paper, following Dwyer *et al.*,[38] the solar helium abundance value of 13.6% shall be used for all calculations.

Dwyer *et al.*[38] also investigated the effects that the ambient planetary magnetic fields have on runaway avalanches in the gas giants. They found that under conditions likely to be present for thunderstorms the magnetic fields have only a minor effect on properties of the runaway avalanches. Only for very low electric fields, near the runaway avalanche threshold $[E_{\mathrm{th}}=(36.1\ \mathrm{kV/m})\times(n/n_o)$ for hydrogen-helium where $n_o=2.69\times10^{25}\ \mathrm{m}^{-3}]$, and only for the case of Jupiter, do the effects of the planetary magnetic field become significant. As shall be discussed below, the electric fields under consideration here are high enough above this threshold (e.g., $E\geq 60\ \mathrm{kV/m}$ at $n=n_o$) that the planetary magnetic fields can be ignored for likely thunderstorm conditions. However, for high altitude discharges, well above the typical thunderstorm heights, the effects of the magnetic fields can become important, so more detailed simulations should be carried out for those circumstances.

Because lightning and, hence, runaway electrons likely occur over a wide range of atmospheric pressures, and in order to aid in the comparison with breakdown in Earth's atmosphere, all results are presented for gas molecular number densities equal to that of air at 1 atm under standard conditions, i.e., $n_o=2.69\times10^{25}\ \mathrm{m}^{-3}$. This density corresponds to a pressure of 0.48 bar in Jupiter.[51] However, no generality is lost here, since all quantities can then be calculated for other gas densities using a simple scaling law as will be explained below.

Using detailed Monte Carlo simulations, Dwyer *et al.*[38] found that the runaway electrons avalanche (e-folding) length for hydrogen-helium at $(n=n_o)$ is well described by the empirical formula, valid over the range ~40–2500 kV/m,

$$\lambda = \frac{6570\ \mathrm{kV}}{(E+(2.91\times10^{-4}\ \mathrm{m/kV})E^2-32.9\ \mathrm{kV/m})}, \qquad (14)$$

where the electric field strength, $E$, is in kV/m (Ref. 38). This expression can be compared with the empirical formula for air given by Eq. (13). For a given electric field, the avalanche length for hydrogen-helium is considerable smaller than for air, due mainly to the lower ionization energy loss rate in hydrogen-helium.

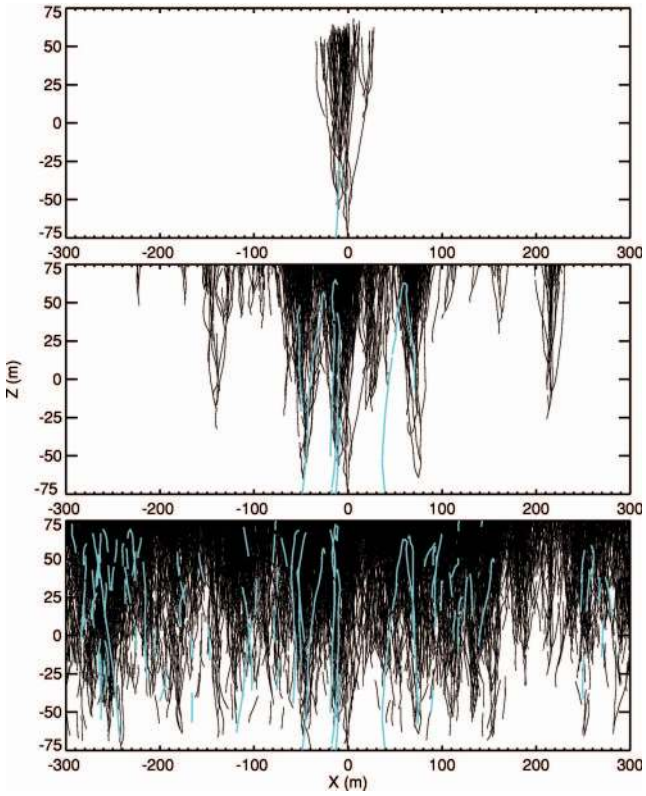


FIG. 2. (Color) Results of the Monte Carlo simulation showing runaway avalanches for air with the electric field $E=750$ kV/m. The black trajectories are individual runaway electrons. The blue trajectories are positrons. The central avalanche is due to the injection of a single, 1-MeV seed electron. All the other avalanches are produced by x-ray and positron feedback. The top panel is for times, $t<0.5\ \mu$s, the middle panel is for $t<2\ \mu$s, and the bottom panel is for $t<10\ \mu$s. If the simulation was not artificially terminated at 10 $\mu$s, the number of runaway electrons would continue to grow indefinitely.

## III. FEEDBACK THRESHOLD AND THE MAXIMUM ELECTRIC FIELD

### A. Results for relativistic feedback

Figure 2 shows an example of runaway electron avalanches for air produced by relativistic feedback. Only the center avalanche was produced by an external (1-MeV) seed energetic electron, e.g., produced by an atmospheric cosmic-ray particle. All the other avalanches are the result of relativistic feedback. The electric field used for this simulation was 750 kV/m over 150 m at standard temperature and pressure (STP), which is about 1 avalanche length longer than is necessary for the runaway electrons to be self-sustaining ($\gamma=1$). This corresponds to a total potential difference slightly over 100 MV. The electric field used in Fig. 2 is at least three times smaller than the conventional breakdown field for clear air and was chosen because at this value the two principal feedback mechanisms (x-ray and positron feedback) are of approximately equal importance, allowing both to be illustrated in one figure. For clarity, only about 1 in 1000 runaway electrons in the simulation (black lines) are actually plotted in Fig. 2. Otherwise, the figure would be too dense with electrons to see individual trajectories. All the positrons are plotted as blue lines. Figure 2 is plotted for

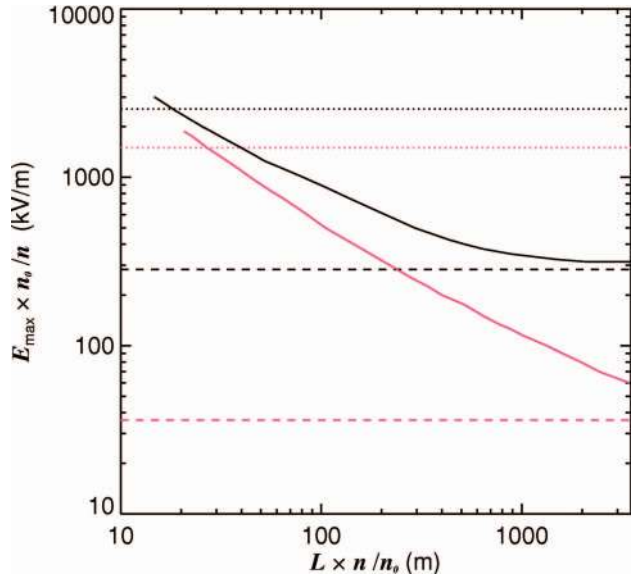


FIG. 3. (Color) The maximum static electric field strength achievable in a hydrogen-helium atmosphere (red) and air (black) vs the length of the electric field region. These lines satisfy the condition for the feedback factor $\gamma=1$. The horizontal dashed lines show the value of the runaway avalanche threshold, $E_{th}$. The horizontal dotted lines show the conventional breakdown thresholds. Above the solid curves, no electric field configuration can be maintained, and therefore the electric field is unstable. Indeed, for configurations in the upper right corner, the electric field is violently unstable. Below the curves and above $E_{th}$, the field may eventually discharge depending upon the ambient cosmic-ray flux and the rate of electrification. Below $E_{th}$, the electric field is stable when the conductivity of air is negligible.

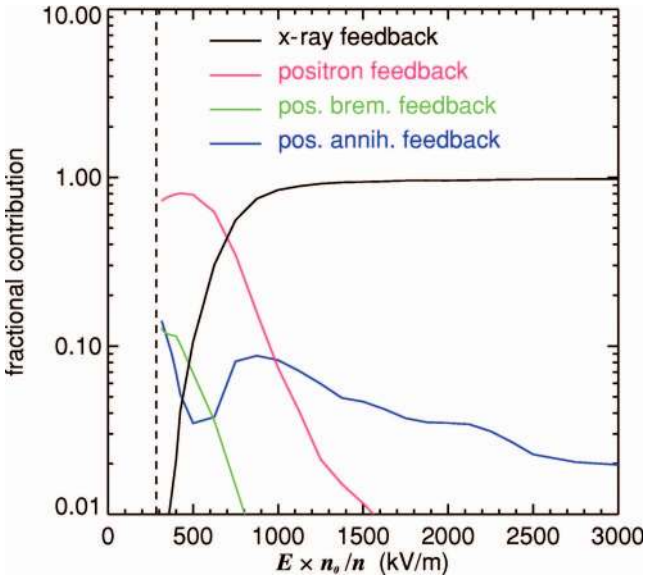


FIG. 4. (Color) Relative contribution to the total feedback from x-ray, positron, positron bremsstrahlung, and positron annihilation feedback for air with $R \gg L$. The vertical dashed line shows the value of the runaway avalanche threshold, $E_{th}$.

three time periods: $t<0.5$ $\mu$s (top panel), $t<2$ $\mu$s (middle panel), and $t<10$ $\mu$s (bottom panel). This figure illustrates the dramatic difference feedback makes over runaway avalanches alone. If feedback did not occur then no additional avalanches would be produced other than the one in the top panel (unless additional seed electrons are introduced). As can be seen, the number of avalanches increases rapidly with time, primarily due to x-ray and positron feedback.

Figure 3 shows the electric field, $E_{max}$, necessary to make $\gamma=1$ (i.e., the condition necessary for self-sustained runaway electron production), as a function of the length of the electric field region, $L$, for hydrogen-helium and air. The results for air were calculated with the latest version of the Monte Carlo, but they are virtually the same as the results first presented by Dwyer,[34] except that the range of values plotted has been extended.

Because the electric fields, plotted in Fig. 3, scale linearly with the gas number density $n$, and the length $L$ scales inversely with $n$, the figure is made independent of number density (and hence the altitude) by plotting $E\times(n_o/n)$ vs $L\times(n/n_o)$, where $n_o=2.69\times10^{25}$ m$^{-3}$ is the number density of air molecules at standard conditions. The results plotted in Figs. 4, 5, 7, 8, and 14 below are also made independent of the gas number density in this way.

It should be noted that the feedback mechanisms continue to work at higher electric field values (shorter distances) than plotted on the left-hand side of Fig. 3. However, these higher values of $E$ exceed the conventional breakdown field, and so it is not clear whether or not such electric field configuration would ever occur in reality. It is possible that during fast transient events, such as lightning, relativistic feedback may occur in this very high field regime. Indeed, the time scale needed for feedback is on the order of a microsecond (see Fig. 8 below), which is shorter than the time needed for conventional streamers to cross the avalanche region. For example, conventional streamers will typically only propagate a few meters per microsecond.[52]

The relative contributions of the four feedback mechanisms discussed in the introduction is shown in Fig. 4. As

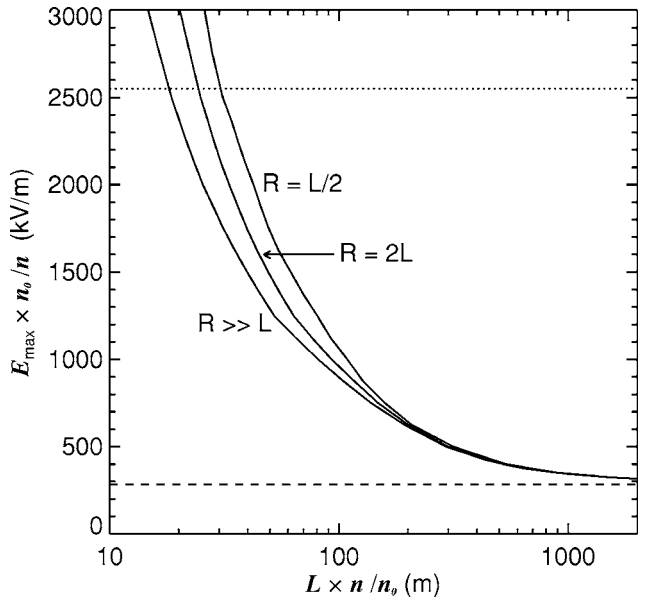


FIG. 5. The maximum static electric field strength achievable in air vs the length of the electric field region for the cases $R=L/2$, $R=2L$, and $R\gg L$. These lines satisfy the condition for the feedback factor $\gamma=1$. The dotted line shows the conventional breakdown threshold and the dashed line shows the runaway avalanche threshold.

can be seen, at high electric field values x-ray feedback dominates. A condition necessary for feedback to occur is that the effective attenuation length (in the electric field direction) of the mediators of feedback, such as the backscattered x rays or the positrons, $\lambda_a$, be greater than the runaway electron avalanche length, $\lambda$. In this way, by increasing the number of avalanche lengths and hence the number of runaway electrons, the number of feedback electrons passing through the midplane can be increased as well, relative to the initial number of runaway electrons. For small electric fields, the avalanche length exceeds the attenuation length of Compton backscattered x rays. As a result, x-ray feedback dies off for fields below about 750 kV/m. On the other hand, the attenuation length due to annihilation of runaway positrons is many hundreds of meters, which allows this mechanism to work down to very low fields. On the other hand, at higher field values the avalanche region is so short that the chance of pair production is small compared with the x-ray feedback probability.

For the Jovian atmospheres, positron feedback is suppressed with respect to x-ray feedback because of the $Z^2$ dependence of the pair-production cross section. As a result, positron feedback does not become important until $E < 100$ kV/m and x-ray feedback dominates over most of the field values plotted in Fig. 3.

In the simulation, x rays were allowed to Compton scatter when outside the avalanche region, potentially returning to the avalanche region to create more runaway electrons. Similarly, positrons created by pair production outside the avalanche region cannot run away, but the 511-keV gamma rays produced by the annihilation can return to the avalanche region. These annihilation photons typically have higher energies than the Compton backscattered photons of x-ray feedback and so their attenuation length is longer. As a result, positron annihilation feedback, although usually smaller than the two principal feedback mechanisms, continues to operate at low field values. Finally, the runaway positrons can on occasion generate bremsstrahlung x rays, which can also produce feedback. This process, like positron annihilation feedback, is smaller than the two principal feedback mechanisms, although it becomes increasingly important at low fields.

One of the most important parameters for determining the feedback threshold is the lateral extent of the avalanche region. This is especially true for x-ray feedback, which results from Compton backscattering. Reducing $R$ compared to $L$ can significantly reduce the amount of x-ray feedback for two reasons: First, a smaller lateral size of the avalanche region means that the solid angle for the backscattered photons to remain in the avalanche region is reduced. Second, for Compton scattering, the larger the backscattering angle, the lower the energy of the scattered x ray. Since higher-energy x rays have a greater probability of producing a secondary electron that will run away, the probability of producing a feedback runaway electron will be greater at larger radial distances where the backscattered photon spectrum is harder. As a result, in order to satisfy the condition $\gamma=1$ for $R$ not large compared with $L$, the number of avalanche lengths must be increased to increase the number of runaway electrons and hence the number of x rays emitted and backscattered. The electric field, $E_{\max}$, necessary to make $\gamma=1$, is plotted in Fig. 5 for three cases: $R \gg L, R=2L$, and $R=L/2$. As before, the electric field is set to zero outside the avalanche region. As can be seen in Fig. 5, for low field values, which are probably the most relevant for thunderstorms, reducing the lateral extent has only a small impact, since the positrons tend to be generated near the initial avalanche. The number of avalanche lengths required for $\gamma=1$ for these three cases will be presented in Sec. V.

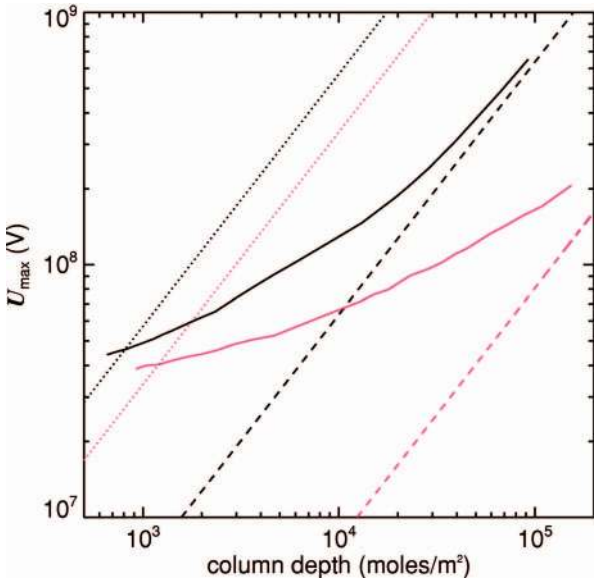


FIG. 6. (Color) The maximum electric potential difference achievable in a hydrogen-helium atmosphere (red) and air (black) vs the gas column depth of the avalanche region (moles/m$^2$). The dotted lines show the conventional breakdown threshold and the dashed lines show the runaway avalanche threshold.

The results in Fig. 3 can be presented in another way that is independent of the gas density and so is more easily applied to other scenarios. This is presented in Fig. 6, which shows the potential difference, $U$, at which $\gamma=1$ (i.e., the maximum possible voltage) versus the gas column depth in the avalanche region. Both quantities are independent of the gas density. As can be seen, the maximum voltages are quite modest and are comparable to voltages inferred for terrestrial thunderstorms. The energy of Jovian lightning bolts has been estimated to be $\sim 10^{12}$ J, much larger than typical terrestrial lightning bolts ($\sim 10^9$ J) (Ref. 50). This result shows that the increased energy cannot be due to greater potential differences in the high field region ($E > 60$ kV/m) and is more likely to result from a larger lateral extent of the discharge region or from an extended low field region.

### B. A simple feedback model

To help understand how relativistic feedback works and to help interpret the more detailed calculations of the Monte Carlo simulations, consider the following simple model. For a uniform electric field, the number of runaway electrons per

energetic seed electron (injected into the start of the avalanche region at $z=0$) that pass through the midplane at $z=L/2$ is $N_{L/2}=\exp(L/2\lambda)$, and the number at the end of the avalanche region at $z=L$ is $N_L=\exp(L/\lambda)$. Let $P_{\mathrm{fb}}$ be the probability that a runaway electron will produce a second generation seed electron near the start of the avalanche region. Then, $P_{\mathrm{fb}}\exp(L/\lambda)$ second generation seed electrons will be created near $z=0$ and these will produce $N_{\mathrm{fb}}=P_{\mathrm{fb}}\exp(L/\lambda)\exp(L/2\lambda)=P_{\mathrm{fb}}\exp(3L/2\lambda)$ feedback electrons at the midplane due to the avalanche multiplication between 0 and $L/2$. [Note in reality and in the Monte Carlo, the next generation seed electrons will be produced throughout the avalanche region and each seed electron will in turn produce $\exp((L/2-z_o)/\lambda)$ runaway electrons at the midplane, where $z_o$ is the creation point of the seed electron. However, for the simple model presented here, this complication will be ignored.] The feedback factor is then found to be $\gamma=N_{\mathrm{fb}}/N_{L/2}=P_{\mathrm{fb}}\exp(L/\lambda)=P_{\mathrm{fb}}N_L$. In other words, $\gamma$ is proportional to the avalanche multiplication factor times the probability that a runaway electron will produce a second generation seed electron. Put another way, in order for the discharge to become self-sustaining (i.e., $\gamma\geq 1$), we require that $P_{\mathrm{fb}}\geq 1/N_L$. Because the amount of avalanche multiplication, $N_L$, can be very large (e.g., $N_L\sim 10\,000$), $P_{\mathrm{fb}}$ may be very small and still result in significant feedback.

The particular value of $P_{\mathrm{fb}}$ depends upon the electric field strength and the length of the avalanche region. For example, the probability of positrons, created in the forward direction, turning around and running away in the backwards direction towards the start of the avalanche region, depends upon the electric field strength, as does the probability of secondary electrons created by backscattered x rays running away. The number of positrons and x rays propagating back to the start of the avalanche region decreases with increasing $L$ due to annihilation of the positrons and attenuation of the x rays, and so $P_{\mathrm{fb}}\propto\exp(-L/\lambda_a)$. Furthermore, $P_{\mathrm{fb}}$ also depends upon the lateral size of the avalanche region as discussed above. However, because $N_L$ is such a sensitive function of $E$ and $L$, depending exponentially on both, if $P_{\mathrm{fb}}$ is reduced by changing a parameter such as $R$, then the condition $\gamma=1$ can usually be maintained if the amount of avalanche multiplication is increased, either by increasing $E$ or $L$.

The above results were calculated for a uniform electric field inside the avalanche region. On the other hand, in reality, electric fields are rarely uniform. However, as long as the electric field remains above the runaway avalanche threshold, $E_{\mathrm{th}}$, at least for air, small variations in the electric field should not substantially change the numerical results above. The reason for this is that the number of runaway electrons at the end of the avalanche region depends only upon the total potential difference across the avalanche region, $U$, and the total gas column depth (i.e., moles/m$^2$) in the avalanche region, $L_n$. This is shown in Eq. (15), which is the number of runaway electrons at $z=L$ per energetic seed electron injected into the start of the avalanche region at $z=0$,

$$N_{\mathrm{RE}}=\exp\left(\int_0^L\frac{dz}{\lambda}\right)=\exp\left(\int_0^L\frac{[E-(2.76\times10^5\ \mathrm{V/m})n/n_o]dz}{7.2\times10^6\ \mathrm{V}}\right)=\exp\left(\frac{U-(6180\ \mathrm{Vm^2/mole})L_n}{7.2\times10^6\ \mathrm{V}}\right).\tag{15}$$

Note that for a given $U$ and $L_n$, $N_{\mathrm{RE}}$ is independent of the specifics of the electric field strength as long as $E$ remains above $E_{\mathrm{th}}$. Therefore, the electric field can vary as a function of position and as long as the average electric field equals the uniform electric field magnitude, $E$, used in the simulation, the number of runaway electrons will be the same. Because the feedback factor, $\gamma$, is most sensitive to $N_{\mathrm{RE}}$, $\gamma$ and hence the $E_{\max}$ curve in Fig. 3 should not change substantially if the electric field is allowed to vary slightly in magnitude as long as the average electric field is the same.

On the other hand, if the variation of $E$ is large, then $P_{\mathrm{fb}}$, defined above, could change substantially. Consequently, the $E_{\max}(\gamma=1)$ curve in Fig. 3 will vary depending upon the details of the electric field, and the exact value should be calculated with Monte Carlo simulations specific for that configuration. However, the basic principles of the four feedback mechanisms do not change when more complicated electric field configurations are involved.

## IV. TIME DEVELOPMENT OF RELATIVISTIC FEEDBACK

### A. Maximum runaway electron flux and discharge times

To understand what happens once relativistic feedback causes the discharge to become self-sustaining and to compare with results of the standard RREA model, consider the case where the electric field strength in air at STP is increased until it obtains a value of $E_o>E_{\max}(L)$, where $L$ is the length of the high field region and $E_{\max}(L)$ is the electric field for which $\gamma=1$. For a uniform field with large lateral extent, $R\gg L$, $E_{\max}(L)$ is given in Fig. 3. For simplicity let us assume that the ambient field is small for $t<0$, with no runaway electrons, and has a constant value of $E_o$ for $t\geq 0$. This may be accomplished either by a fast charging mechanism or during a nonuniform discharge in which the field is enhanced locally due to the charge motion. For very rapid increases in the electric field to occur inside thunderstorms, the latter scenario is more plausible. Indeed, Dwyer[37] calculated how such rapid enhancements can occur under normal thunderstorm conditions.

Let $S_o$ be the flux of energetic seed particles that run away, e.g., the flux due to atmospheric cosmic-ray particles and radioactive decays. Depending upon the altitude and the geographic location,[53] $S_o$ is in the range 100–10 000 m$^{-2}$ s$^{-1}$. The value $S_o\sim 1000$ m$^{-2}$ s$^{-1}$ will be used for the calculations presented here. Under these conditions the effects of positive feedback will cause the number of runaway electrons to grow rapidly with an e-folding time $\tau'$ defined above in Sec.

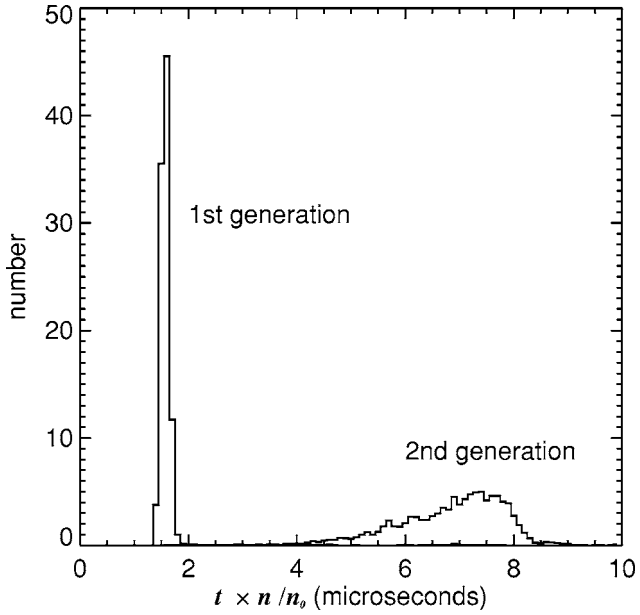


FIG. 7. Time distribution of runaway electrons entering the midplane in the avalanche region for $E=350\ \mathrm{kV/m}\times(n/n_o)$. The left distribution is the initial runaway electron avalanche initiated at time $t=0$. The right distribution is the arrival times of the next generation (from feedback) runaway electrons.

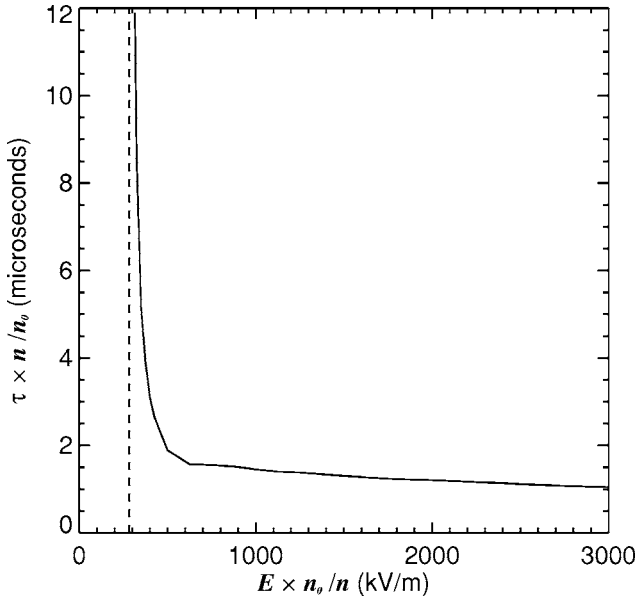


FIG. 8. The average time between successive generations of electrons, $\tau$, as a function of electric field strength. The vertical dashed line shows the value of the runaway avalanche threshold, $E_{\mathrm{th}}$.

II. If no feedback were occurring then the flux of runaway electrons, according to the RREA model,[33] at the end of the avalanche region, would be

$$F_{\mathrm{RREA}} = S_o \exp(\xi), \quad \text{where } \xi = \int_0^L \frac{dz}{\lambda}. \tag{16}$$

In Eq. (16), $\xi$ is the number of e-folding lengths and is equal to $L/\lambda$ for a uniform field.

When relativistic feedback is considered, then the runaway electron flux at time $t$ is the sum of all the feedback generations up until that time,

$$F_{\mathrm{RF}} = \sum_{n=0}^{t/\tau} F_n(t), \tag{17}$$

where $F_n(t)$ stands for the flux of the $(n+1)^{th}$ runaway electron generation and is given by the recursion relation

$$F_{n+1}(t) = \gamma \int_0^t D(t-t')F_n(t')dt', \tag{18}$$

where $D(t-t')$ is the transfer function that takes a particle entering the midplane at time $t'$ and gives the normalized distribution of the next generation of particles entering the midplane. An example of the distribution $D(t-t')$ for a field $E=350\ \mathrm{kV/m}\times(n/n_o)$ is shown in Fig. 7. The average time between successive generations of runaway electrons, $\tau$, as a function of electric field strength is shown in Fig. 8.

In Eqs. (17) and (18), $F_0=F_{\mathrm{RREA}}$, given by Eq. (16). For simplicity, if we ignore the time dispersion and use the approximation $D(t-t')=\delta(t-\tau-t')$, where $\delta$ is the Dirac delta function, then

$$F_n = \gamma^n S_o \exp(\xi)\theta(t-n\tau), \tag{19}$$

where $\theta$ is the step function. Plugging this expression into that for $F_{\mathrm{RF}}$ gives

$$F_{\mathrm{RF}} = S_o \exp(\xi)\sum_{n=0}^{t/\tau} \gamma^n. \tag{20}$$

Using the following for the summation

$$\sum_{n=0}^{t/\tau} \gamma^n = \begin{cases} \dfrac{(\gamma^{(t/\tau)+1}-1)}{(\gamma-1)}, & \gamma \neq 1 \\ (t/\tau)+1, & \gamma = 1, \end{cases} \tag{21}$$

the runaway electron flux resulting from relativistic feedback for the case $t \gg \tau$, which is the regime of interest here, is then

$$F_{\mathrm{RF}} = \begin{cases} S_o \exp(\xi)\exp(t/\tau')/(\gamma-1), & \gamma > 1 \\ S_o(t/\tau)\exp(\xi), & \gamma = 1 \\ S_0 \exp(\xi)/(1-\gamma), & \gamma < 1, \end{cases} \tag{22}$$

where

$$\tau' \equiv \tau/\ln(\gamma) \tag{23}$$

is the e-folding time to increase the flux of runaway electrons due to feedback (assuming $\gamma>1$). Note that for $\gamma>1$ and a uniform electric field, Eq. (22) is proportional to $\gamma^{t/\tau}\exp(L/\lambda)$, which is the same as Eq. (2) in Dwyer.[34] Furthermore, for the case $\gamma \ll 1$, i.e., very little feedback, $F_{\mathrm{RF}}$ approaches the standard result for the RREA model given by Eq. (16).

It should be noted that relativistic feedback also operates when $\gamma<1$, as can be seen in Eq. (22). In this case, the discharge does not become self-sustaining. However, the effect of the feedback can dramatically increase the number of runaway electrons produced per seed particle injected as $\gamma$ approaches one.

On the other hand, for $\gamma > 1$, the discharge becomes self-sustaining and increases exponentially with time. Comparing Eqs. (16) and (22) (for $\gamma > 1$), the ratio of the runaway electron flux from relativistic feedback to that from the RREA model is then

$$\frac{F_{\mathrm{RF}}}{F_{\mathrm{RREA}}} \approx \frac{\exp(t/\tau')}{(\gamma - 1)}. \tag{24}$$

Equation (24) is also the ratio of x rays emitted by the two mechanisms, since the x-ray emission is proportional to the flux of runaway electrons.

To see how much larger the runaway electron (and x-ray) flux from relativistic feedback can be compared with the standard RREA model we must know how long the feedback continues. As an estimate, it will be assumed that the feedback continues until the time is reached when the ambient electric field, $E$, collapses due to the large amount of ionization generated by the runaway electrons.

In a one-dimensional, plane geometry, the change in the electric field is given by

$$\frac{dE}{dt} = -\frac{e}{\varepsilon_o}(n_e\alpha_e + n_-\alpha_- + n_+\alpha_+)E, \tag{25}$$

where $n_e$ is the number density of the free low-energy electrons produced by ionization of the gas; $n_+$ is the number of positive ions and $n_-$ is the number of negative ions produced when the electrons attach to oxygen and water molecules; $\alpha_e = 9.4 \times 10^{-2}$ m$^2$/V s, $\alpha_+ = 1.4 \times 10^{-4}$ m$^2$/V s, and $\alpha_- = 1.9 \times 10^{-4}$ m$^2$/V s are the corresponding mobilities of the charged particles. In this simple calculation, the current produced directly by the runaway electrons is ignored, since it is much smaller than from the drifting low-energy electrons and the ions. The number densities are given by the following equations:

$$\frac{dn_e}{dt} = I_e F_{\mathrm{RF}} - \frac{n_e}{\tau_a}, \tag{26}$$

$$\frac{dn_-}{dt} = \frac{n_e}{\tau_a}, \tag{27}$$

$$\frac{dn_+}{dt} = I_e F_{\mathrm{RF}}, \tag{28}$$

where $I_e$ is the average ionization per unit length of runaway electrons moving through the gas. For air at STP, $I_e \sim 9000$/m for the cases under consideration here. $\tau_a$ is the attachment time of free low-energy electrons, principally, to oxygen and water vapor. $\tau_a$ is a rather complicated function of electric field strengths, gas density, and composition. For air at STP, $\tau_a \sim 10^{-8}$ s.

Using Eq. (22) ($\gamma > 1$) for $F_{\mathrm{RF}}$, Eqs. (26)–(28) have the solutions

$$n_e = \frac{\tau_a I_e F_{\mathrm{RF}}}{\left(1 + \frac{\tau_a}{\tau'}\right)}, \tag{29}$$

$$n_- = \frac{\tau' I_e F_{\mathrm{RF}}}{\left(1 + \frac{\tau_a}{\tau'}\right)}, \tag{30}$$

$$n_+ = \tau' I_e F_{\mathrm{RF}}. \tag{31}$$

Substituting Eqs. (22) (for $\gamma > 1$) and (29)–(31) into Eq. (25) and integrating gives the value of the electric field at the end of the avalanche region

$$E = E_o \exp(-\kappa(t)), \quad \text{where}$$
$$\kappa(t) = \frac{I_e \alpha' e S_o \tau'^2 \exp(\xi)\exp(t/\tau')}{(\gamma - 1)\varepsilon_o}. \tag{32}$$

Here the quantity $\alpha'$ is the effective mobility and is given by

$$\alpha' = \frac{\alpha_e}{\left(1 + \frac{\tau'}{\tau_a}\right)} + \frac{\alpha_-}{\left(1 + \frac{\tau_a}{\tau'}\right)} + \alpha_+. \tag{33}$$

The discharge time, $t_{\mathrm{dis}}$, is defined as the time needed to reduce the field at the end of the avalanche region by $e^{-1}$. This is found by solving $\kappa(t_{\mathrm{dis}}) = 1$ in Eq. (32) for $t_{\mathrm{dis}}$. The result is

$$t_{\mathrm{dis}} = \tau' \ln\left(\frac{(\gamma - 1)\varepsilon_o}{I_e \alpha' e S_o \tau'^2 \exp(\xi)}\right). \tag{34}$$

The condition $\kappa(t) = 1$ also gives the value of Eq. (24), the ratio of the runaway electron flux from relativistic feedback to that from the standard RREA model alone at time $t_{\mathrm{dis}}$,

$$\frac{F_{\mathrm{RF}}}{F_{\mathrm{RREA}}} = \frac{\varepsilon_o}{I_e \alpha' e S_o \tau'^2 \exp(\xi)}. \tag{35}$$

The evaluation of this equation is simplified slightly by using the results from the simple model in Sec. III above. The feedback rate for $\xi$ avalanche lengths is approximately equal to

$$\gamma \sim \exp((\xi - \xi_o)(1 - \lambda/\lambda_a)), \tag{36}$$

where $\xi_o$ is the number of avalanche lengths that occur when $\gamma = 1$ for the same electric field strength, $E$. Here, $\lambda/\lambda_a$ is the ratio of the runaway avalanche length to the effective attenuation length of the mediators of the feedback (i.e., the runaway positrons or the backward propagating energetic photons) and takes into account the change in $P_{\mathrm{fb}}$ due to the extra propagation length experienced by the feedback mediators for different $\xi$. For feedback to occur $\lambda < \lambda_a$. Indeed, for most cases $\lambda \ll \lambda_a$. As a result, Eq. (36) can be approximated with $\gamma \sim \exp(\xi - \xi_o)$. Using this result, Eq. (23) then gives $\tau' \sim \tau/(\xi - \xi_o)$. Plugging this expression into Eq. (35) gives a $\xi$ dependence of the form $(\xi - \xi_o)^2/\exp(\xi)$, which has a maximum at $(\xi - \xi_o) = 2$.

In addition, if the length of the avalanche region is changed, then the time, $\tau$, will change as well. For positron feedback, $\tau \propto L/L_o$, where $L_o$ is the length of the avalanche region when $\gamma = 1$. For x-ray feedback, the dependence of $\tau$ on $L$ is more complicated and depends upon the specific

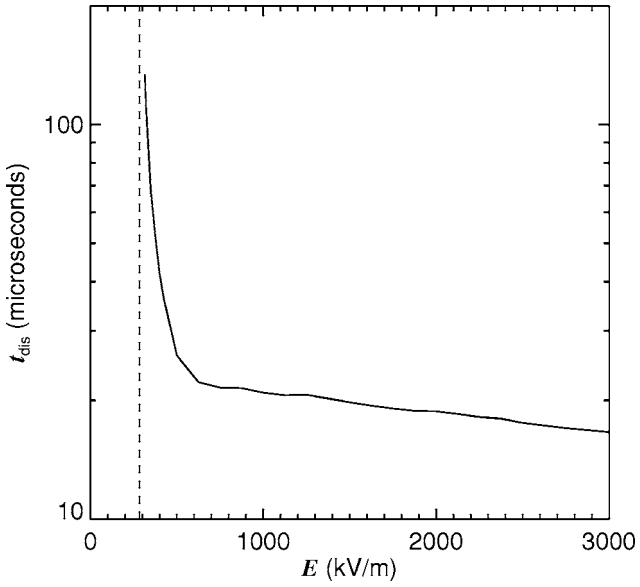


FIG. 9. The discharge time for relativistic feedback at STP. This is the time needed to reduce the electric field at the end of the avalanche region by $1/e$. The vertical dashed line shows the value of the runaway avalanche threshold, $E_{th}$.

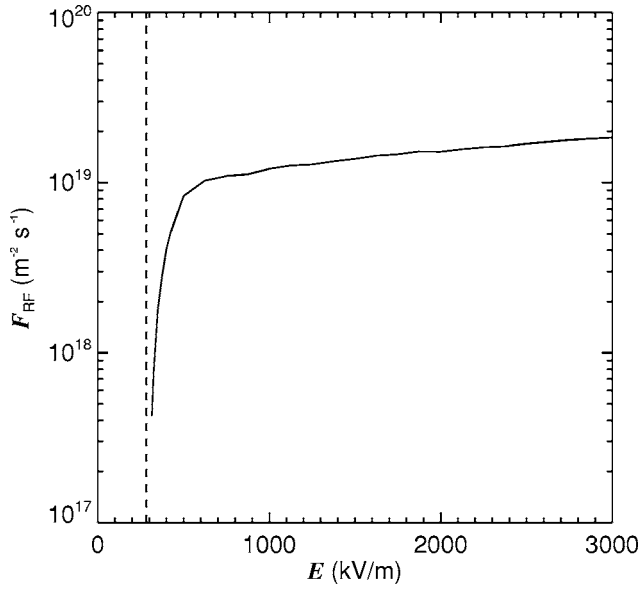


FIG. 11. The maximum runaway electron flux from relativistic feedback vs electric field strength at STP, assuming that relativistic feedback ceases at time $t_{dis}$. Since the mean free path for emitting bremsstrahlung is on the order of 100 m, which is comparable to the avalanche length, this flux should be approximately equal to the x-ray flux as well. The vertical dashed line shows the value of the runaway avalanche threshold, $E_{th}$.

geometry of the avalanche region. However, as long as the difference between $L$ and $L_o$ is not too large, $\tau$ will only change by a factor on the order of unity and so such differences will be ignored for the following calculations.

Figures 9 and 10 show Eqs. (34) and (35), respectively, for the case $(\xi-\xi_o)=2$ at STP. As can be seen in Fig. 10, relativistic feedback increases the flux over the RREA model by several trillion in some cases. The peak flux, $F_{RF}$, at STP is also plotted in Fig. 11.

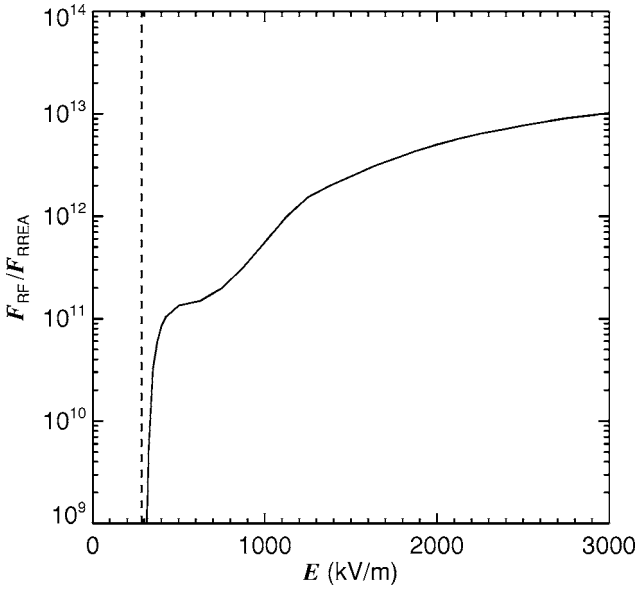


FIG. 10. The ratio of the maximum runaway electron (and x-ray) flux from relativistic feedback to that from the standard RREA model vs electric field strength at STP, assuming that relativistic feedback ceases at time $t_{dis}$. The vertical dashed line shows the value of the runaway avalanche threshold, $E_{th}$.

As can be seen in Fig. 9, $t_{dis}$ is extremely short, especially when compared to charging times scales (e.g., a few tens of seconds) that are likely to occur in nature.[31] Indeed, relativistic feedback can discharge the large-scale electric field in some cases faster than lightning can discharge the field.

The electrical current density generated by the discharge at time $t_{dis}$ is

$$J=\frac{\varepsilon_o E}{\tau'}. \tag{37}$$

The maximum current density at STP is plotted in Fig. 12. For the radius $R=100$ m, the minimum current necessary to maintain the electric field at time $t_{dis}$ is almost 10 kA, which would need to be applied across a minimum of $\sim$10 MV. Such large currents can be supplied by lightning discharges and may be possible under laboratory conditions, but only briefly. Even if large enough external current could be supplied momentarily to maintain the electric field, the discharge current would continue to rise exponentially until it would become impossible to supply enough current to prevent the field collapse. For this reason, the $E_{max}$ (and $U_{max}$) curves presented above can be considered the upper limit on the uniform, static electric field achievable in the air and in hydrogen-helium.

In contrast, using Eq. (16) for the RREA model in the above calculation gives the discharge time for the RREA model alone,

$$t_{RREA}=\left\{\frac{2\varepsilon_o}{I_e(\alpha_+ + \alpha_-)eS_o \exp(\xi)}\right\}^{1/2}. \tag{38}$$

For the same conditions used in Fig. 9, the time, $t_{RREA}$, is between about 1 and 10 sec, much longer than the discharge

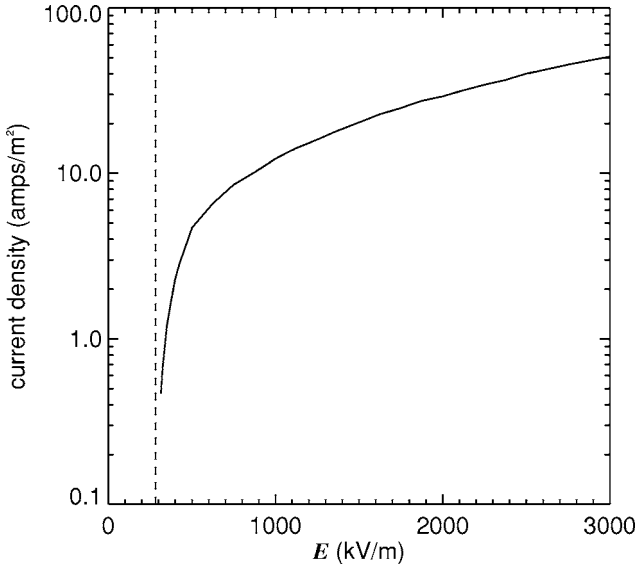


FIG. 12. Maximum electric current density generated by relativistic feedback vs electric field strength at STP for an avalanche region with $R \gg L$, assuming that relativistic feedback ceases at time $t_{\mathrm{dis}}$. The vertical dashed line shows the value of the runaway avalanche threshold, $E_{\mathrm{th}}$.

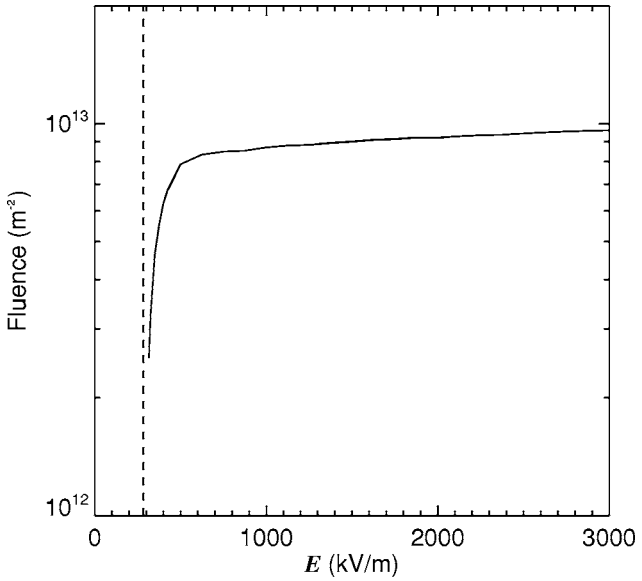


FIG. 13. Fluence of runaway electrons generated by relativistic feedback vs electric field strength at STP, assuming that relativistic feedback ceases at time $t_{\mathrm{dis}}$. This fluence should be approximately equal to the x-ray fluence as well. The vertical dashed line shows the value of the runaway avalanche threshold, $E_{\mathrm{th}}$.

time for relativistic feedback. Furthermore, the discharge time for the RREA model is comparable to charging times for thunderstorms, so, unlike relativistic feedback, the RREA model alone will not guarantee that the field will collapse. Therefore, the runaway avalanche threshold field, $E_{\mathrm{th}} = 36.1\ \mathrm{kV/m} \times (n/n_o)$ for hydrogen-helium and $E_{\mathrm{th}} = 284\ \mathrm{kV/m} \times (n/n_o)$ for air, does not place a limit on the static electric field, since the ionization rate produced by the runaway avalanches alone is not necessarily sufficient to discharge the field under conditions of active electrification. Indeed, electric fields are often measured in terrestrial thunderstorms to be well above this value.[54] This argument especially holds true for Jovian thunderstorms, which are much deeper in the planetary atmospheres, and so the injection rate of energetic seed particles by cosmic ray is substantially reduced.[55]

Integrating Eq. (22) (for $\gamma > 1$) gives the fluence (number per unit area) of runaway electrons generated by relativistic feedback at time $t_{\mathrm{dis}}$,

$$N_{\mathrm{RD}} = F_{\mathrm{RD}}\tau' = \frac{\varepsilon_o}{I_e \alpha' e \tau'}. \tag{39}$$

Equation (39) is plotted in Fig. 13 for the case $(\xi - \xi_o) = 2$ at STP. The total number of runaway electrons generated by relativistic feedback throughout the avalanche region is obtained by multiplying Eq. (39) by the area of the avalanche region. Since this area may potentially be measured in square kilometers inside thunderstorms, the total number of runaway electrons generated may be enormous.

### B. Nonuniform discharges

In the above calculations it was assumed that relativistic feedback is terminated once the electric field at the end of the avalanche region is reduced. For a uniform avalanche region with no lateral variation this will be the case. However, in a realistic discharge, the electric field will not be exactly uniform. As a result, the discharge from both the RREA model and the relativistic feedback mechanism will be largest in some region, which will be discharged first. Dwyer[37] showed that under such conditions the electric field in the remaining avalanche region—in front of the discharged region—will be locally enhanced resulting in more runaway avalanches and allowing the feedback to continue. This can be understood by considering Fig. 6, which shows the potential difference necessary for a self-substantiated discharge ($\gamma = 1$) versus the gas column depth of the avalanche region. Consider a localized discharge at the end of the avalanche region due to the large number of runaway electrons generated. If the initial column depth of the avalanche region is $L_n$, then the remaining avalanche region (with $E > E_{\mathrm{th}}$) after the discharge of the field at the end will have a column depth, $L_n'$, with a total potential difference of $U'$. Depending on how completely the electric field at the end of the avalanche region is discharged, it is entirely possible for the point $[L_n', U']$ to be above the $U_{\max}$ curve in Fig. 6 with a larger feedback factor, $\gamma$, than before the discharge. As the discharge due to relativistic feedback continues, the potential difference remaining in the avalanche region will follow a trajectory in the $U$ versus column depth plot, starting from the upper right corner and progressing to the left in Fig. 6. If the discharge was perfect and completely reduced the electric field to zero then the trajectory would be a horizontal line. For a realistic discharge the potential difference will decrease from right to left. However, it is possible for the potential difference of the avalanche region to stay above the $U_{\max}$ curve given in Fig. 6 throughout the entire discharge. This would allow the flux $F_{\mathrm{RF}}$ to continue to increase, producing even more runaway electrons and larger discharge currents. As a result, the number of

runaway electrons produced by relativistic feedback and the increase over the RREA model may be even larger than estimated by Eqs. (35) and (39).

Finally, Dwyer[37] used a combination of Monte Carlo simulations and runaway electron transport equations to model such a discharge and found that in the manner described above, an ordinary RREA discharge can result in the $\gamma=1$ curve being crossed and the discharge to become self-sustaining as presented in this section. Furthermore, Dwyer[37] showed that this localized enhancement in the electric field may become large enough to initiate lightning.

### C. The effects of the self-generated magnetic field

Using Ampere's law and Eqs. (22) (for $\gamma>1$) and (29)–(31) above, the azimuthal magnetic field at radius $r$ generated by the runaway electrons and the drifting low-energy electrons and ions is found to be approximately

$$B=\frac{\mu_o\tau' I_e\alpha' eS_o\exp(\xi)\exp(t/\tau')Er}{2(\gamma-1)}, \tag{40}$$

where the contribution of the runaway electrons to the current is ignored. This approximation is justified since the current from the runaway electron motion is small compared to that from the drifting electrons and ions. Plugging Eq. (34) in Eq. (40) gives the maximum magnetic field produced by relativistic feedback,

$$B_{\max}=\frac{RE}{2\tau' c^2}\approx\frac{RE}{\tau c^2}, \tag{41}$$

occurring at $r=R$, the lateral radius of the avalanche region.

The Lorentz force on the runaway electrons can be ignored when $cB\ll E$. This condition holds throughout the relativistic feedback discharge as long as $R\ll\tau c$. Multiplying the curve in Fig. 8 by the speed of light shows that this condition is generally met and that $\tau c$ ranges from about 4000 m down to about 300 m as the electric field goes from the lowest to the highest values. Because the length of the avalanche region also decreases rapidly with $E$, the condition that $R\gg L$ used in the earlier calculations remains valid. However, even if $R\gg L$ were violated this does not mean that relativistic feedback no longer applies. It simply means that the $\gamma=1$ curve would need to be recalculated for that specific geometry. In summary, the magnetic field generated by the relativistic feedback, while substantial, does not change the results derived in this paper.

## V. DISCUSSION

### A. Fluence of runaway electrons

The limit on the electric field set by relativistic feedback (e.g., as plotted in Fig. 5) has a profound implication for the electrical properties of thunderstorms and runaway avalanche development. Figures 3 and 5, along with the avalanche length, λ, can be used to calculate the maximum possible runaway electron avalanche multiplication, $\exp(\xi)$. This is plotted in Fig. 14. As can be seen, under no conditions does $\exp(\xi)$ exceed $10^5$ for air, and in this extreme case, the size of the avalanche region is so large that it may no longer be applicable to thunderstorms (recall distances scale inversely with density so at thunderstorm altitudes, the lengths plotted in Fig. 5 are several times longer).

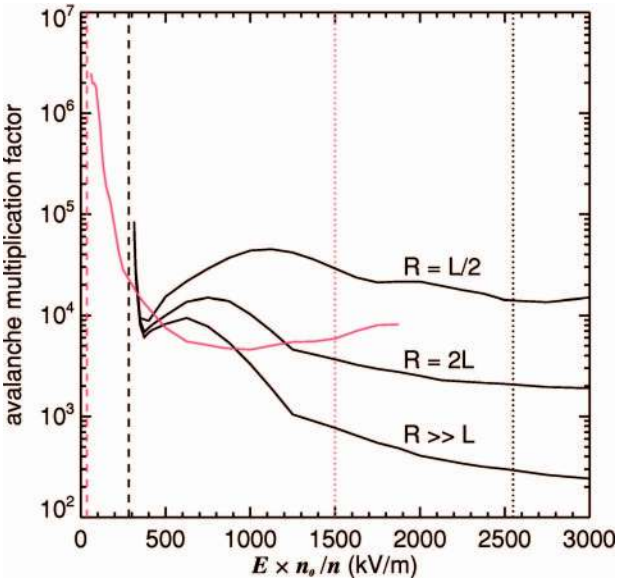


FIG. 14. (Color) Maximum possible runaway electron avalanche multiplication factor $\exp(\xi)$ vs electric field strength for air (black) for the cases $R=L/2$, $R=2L$, and $R\gg L$. For comparison, the maximum possible runaway electron avalanche multiplication factor for hydrogen-helium with $R\gg L$ is also presented (red). The vertical dashed lines show the value of the runaway avalanche threshold, $E_{\text{th}}$. The vertical dotted lines show the conventional breakdown thresholds.

Runaway avalanches have a long history of being used by theoreticians to explain a variety of phenomena in the atmospheric sciences, including sprites, narrow bipolar radio pulses, lightning initiation, and terrestrial gamma-ray flashes. In the past, all of these applications of the RREA model required very large avalanche multiplication. As a result, Fig. 14 places a severe constraint on such models. For example, for lightning initiation models that use extensive cosmic-ray air showers in conjunction with the RREA model,[56] this limit on the avalanche multiplication along with the lateral diffusion of the runaway avalanches prevents even large air showers from having a significant effect on the electrical environment of the thundercloud.[37] A similar problem occurs for narrow bipolar pulses (NBPs).[57] For models involving the simultaneous action of extensive cosmic-ray air showers and the RREA model,[58] it will be difficult to account for the very large radio emission of the narrow bipolar pulses when the avalanche multiplication is limited to $10^5$.

On the other hand, the fluence of runaway electrons from relativistic feedback (Fig. 13) is very large and has an interesting value. Dwyer and Smith[29] estimated that the total number of runaway electrons at the source of TGFs must be between $10^{16}$ and $10^{17}$, depending upon the altitude of the source. In order to get $10^{17}$ runaway electrons, for most of the range plotted in Fig. 13, the avalanche region must have an area of about $10^4$ m$^2$, which is only about 100 m across. Such a high field region is reasonable for thunderstorms, which can measure many kilometers across. Furthermore, a discharge time of 17–134 $\mu$s, as seen in Fig. 9, corresponds

to a discharge time of approximately 0.1–1 ms, at 15 km. This rise time in the number of runaway electrons is consistent with the rise times often seen in TGFs.

### B. The Jovian atmospheres

In terms of the number of avalanche lengths needed for feedback to become important, in many cases more e-folding lengths are required for the Jovian atmospheres than for air (see Fig. 14). This is mainly due to the $Z^2$ dependence of the bremsstrahlung cross section, thus requiring more runaway electrons in low-$Z$ atmospheres in order to emit the same number of x rays. On the other hand, the avalanche lengths for the Jovian atmospheres are generally shorter than for air,[38] so the length scales needed for feedback are shorter for hydrogen-helium at the same electric field magnitudes (see Fig. 3).

Because thunderstorms in the Jovian planets are thought to occur deep in the atmospheres, e.g., $p>2$ bar for Jupiter and $p>10$ bar for Saturn, extensive air showers will be well past the shower maximum at these pressures and so the number of energetic particles injected into the avalanche regions will be much smaller than for Earth. As a result, if runaway electrons do play a role in thunderstorm and lightning processes in the Jovian atmospheres, they may require the relativistic feedback mechanism.

The conventional breakdown field for the Jovian atmospheres has been estimated to be about 1500 kV/m for a clear atmosphere and about a factor of 3 lower when hydrometeors are present.[32] For example, based upon estimates of the ionization rate in hydrogen compared with nitrogen, Yair *et al.*[59] argued that the breakdown field for molecular hydrogen should be 2.3 times lower than for nitrogen.[59] They then lowered the breakdown field by a factor of 3 to include effects from hydrometeors, concluding that the breakdown field is about 1000 kV/m at 2 bar in Jupiter's atmosphere. This corresponds to a breakdown field of about 400 kV/m at $n=2.69\times10^{25}$ m$^{-3}$, which is a factor of 10 larger than the runaway avalanche threshold field and well within the range of electric fields under consideration here. It should be noted, however, that it is largely speculation that the presence of hydrometeors will lower the breakdown field, resulting in a hot leader channel (i.e., lightning), and not simply discharge the electric field due to increased coronal emission.

### C. A new gas breakdown mechanism

The above calculations showed that the effects of feedback as reported by Dwyer[34,37] can increase the flux of runaway electrons and the accompanying x-ray emission by factors of trillions, resulting in large charge motion, an increase in the conductivity, and ultimately, the collapse of the ambient electric field under conditions for which ordinary runaway breakdown has a completely negligible effect. Because of the dramatic differences in the discharge properties and the difference in the key mechanism involved, it is proposed that the feedback mechanism constitutes a unique and separate discharge mechanism from runaway electron avalanches alone. The situation is similar to the difference between a low-energy electron avalanche in a gas and the Townsend breakdown, which proceeds via a feedback mechanism involving low-energy ions and UV photons. In a gas, when the number of electrons moving in an electric field, created by ionization, grows with time this process is called "avalanche multiplication." This is the principle behind gas proportional counters.[60] Electron avalanches are not considered a breakdown phenomenon because they are driven by external sources of seed electrons. The RREA model is the high-energy analog of low-energy avalanches. For example, no one would say a gas proportional counter, operating normally in the proportional regime, is undergoing gas breakdown. Indeed, the RREA model also is operating in the proportional regime, since the ionization generated is proportional to the number of energetic seed particles provided by the external source.

For a conventional discharge, when the voltage is increased a new phenomenon occurs: Optical (UV) and ion feedback make the discharge become self-sustaining and there is an abrupt transition to a new state called a "Townsend breakdown."[49,61] The Townsend breakdown is self-sustaining, the first key requirement for a discharge to be considered a gas breakdown.[61] The Townsend breakdown also results in the collapse of the electric field, the second criteria for breakdown, and in effect sets a limit on the electric field for a given gas and geometry, just as with relativistic feedback. As with the Townsend breakdown, the discharge produced by relativistic feedback becomes self-sustaining and rapidly collapses the electric field once the feedback factor, $\gamma$, is greater than 1. Therefore, it is a true gas breakdown and is an independent mechanism from normal runaway electron avalanches (RREA model), just as the Townsend breakdown is considered an independent mechanism from ordinary electrons avalanche multiplication. Finally, even though the principal difference between relativistic feedback and the RREA model is the addition of the backward propagating photons and positrons, the effect of adding these two new components is profound, resulting in a completely different behavior of the discharge. In a similar way, the addition of one new component to Wilson's original runaway electron model,[62] namely, secondary electron production from Møller scattering, had profound effects resulting in the familiar RREA model, which is distinct from Wilson's original model.

The RREA model is often and erroneously referred to as "runaway breakdown." However, by several criteria, the so-called runaway breakdown is not a true gas breakdown. Following the standard definitions of a gas breakdown from classical discharge physics, a breakdown should represent a new internal state of the system and should not be driven by external influences. For the RREA model, if the external supply of energetic seed electrons is cut off then the runaway avalanches will abruptly stop. Second, the breakdown should act to collapse the electric field unless large external currents are applied. The RREA model under most circumstances simply increases the conductivity of the gas medium but does not necessary lead to the collapse of the electric field.

Because the term runaway breakdown, even though a misnomer, is already strongly tied to the RREA model, it is proposed that relativistic feedback, when in the $\gamma>1$ regime,

be referred to as relativistic breakdown, since the mechanism involves particles moving at or near the speed of light. Alternatively, the term "high-energy" could be adopted. However, the term high energy is already used in the field of discharge physics to describe high-energy content phenomena such as electrical arcs.

### D. Development of a plasma

Two of the basic requirements for an ionized gas to be considered to be a plasma are that the Debye length, $\lambda_D = (\varepsilon_o k T_e / n_e e^2)^{1/2}$, be much smaller than the size of the system, and that many free electrons are contained within the Debye volume,[61] $4\pi\lambda_D^3/3$. Using the flux of runaway electrons shown in Fig. 11 along with Eq. (29) gives a peak low-energy electron density of $\sim 10^{14}$ m$^{-3}$ for relativistic feedback over most of the electric field strengths considered. Using a typical electron temperature of a few eV for electrons drifting in an electric field gives $\lambda_D \sim 10^{-3}$ m, so clearly these conditions for the ionized gas to be considered a plasma are easily satisfied. On the other hand, for the same number of avalanche lengths, the RREA model produces a runaway electron flux less than $10^8$ m$^{-2}$ s, which leads to an electron density of only $10^4$ m$^{-3}$. This gives a Debye length of 100 m, and so the condition that the size of the system is much larger than the Debye length is not satisfied in this case. Therefore, unlike relativistic feedback, the ionized gas resulting from the RREA model alone will not produce a plasma.

### E. Relativistic breakdown in the laboratory

Finally, while this paper was presented with atmospheric processes in mind, applications of relativistic feedback and relativistic breakdown to astrophysical and laboratory situations should be kept in mind. For the electrostatic case, the primary obstacle to laboratory experiments on relativistic breakdown is the large electrostatic potential needed. For example, for hydrogen-helium, at fields just below the conventional breakdown field, this potential is about 40 MV (see Fig. 6). Such a potential difference should be possible in the laboratory. For example, the Brookhaven National Laboratory Tandem Accelerator currently has two electrostatic generators that operate at voltages up to ±15 MV, allowing for the total potential difference of 30 MV. Relativistic feedback and relativistic breakdown should occur in most gases—although the effects in higher-$Z$ gases require further study—and so highly electronegative gases could also be used. In addition, it is possible to reduce the required potential by optimizing the geometry. For example, a geometry with two or more connected avalanche regions with opposite electric field vectors would allow x rays from one avalanche region to directly produce, with no need to backscatter, secondary avalanches in the opposite region, and vice versa. Positrons in one region could also be produced by x rays from the other region. Such positrons would run away with a significantly higher efficiency, since they would be created with velocities in the correct direction to run away and would not need to turn around. Such feedback might be descriptively called "cross-fire feedback." In fact, balloon soundings in thunderstorms show that such electric field configurations do occasionally exist inside thunderstorms.[31] For such configurations the $U_{\max}$ curve in Fig. 6 is reduced for a given column depth of each avalanche region and the required potential difference is therefore reduced. In the laboratory, one might imagine a high pressure gas to reduce the physical dimensions required with perhaps a cylindrical or spherical cross-fire geometry, e.g., with electric field vectors pointed radially outward. Alternatively, a transient electric field may also generate relativistic breakdown if the high field lasts longer than the feedback time. For high pressures, the feedback time may be reduced to a fraction of a microsecond. If a system to generate relativistic breakdown in the laboratory could be realized, then the fluxes of high-energy electrons and x rays produced would be mainly limited by the amount of current that could be supplied to maintain the electric field, and so these fluxes could in principle be extremely large. Such experiments would be very interesting, since they would explore a fundamentally new breakdown mechanism, common to many gases, that has never before been studied.

### F. Summary

In this paper, a detailed study of the new gas breakdown mechanism introduced by Dwyer[34] has been carried out. It has been found that this mechanism can produce dramatic ($\times 10^{13}$) increases in the flux of runaway electrons over the standard relativistic runaway electron avalanche model[33] and sets a limit on the static electric field that can be maintained in gaseous media. Because this mechanism is a true electrical breakdown involving relativistic runaway electrons that is distinct from the RREA model, the name "relativistic breakdown" is proposed for this new mechanism. Relativistic breakdown may play a role in terrestrial gamma-ray flashes and may be important for understanding thunderstorm and lightning processes on Earth as well as on the Jovian planets.

## ACKNOWLEDGMENTS

This work was supported by the NSF under Grant No. ATM 0133773.

[1] M. Bakhtiari, G. J. Kramer, and D. G. Whyte, Phys. Plasmas **12**, 102503 (2005).
[2] R. Yoshino, T. Kondoh, Y. Neyatani, K. Itami, Y. Kawano, and N. Isei, Plasma Phys. Controlled Fusion **39**, 313 (1997).
[3] H. Knoepfel and D. A. Spong, Nucl. Fusion **19**, 785 (1979).
[4] J. R. Martín-Solís and R. Sánchez, Phys. Plasmas **13**, 012508 (2006).
[5] H. Smith, P. Helander, L.-G. Eriksson, and T. Fülöp, Phys. Plasmas **12**, 122505 (2005).
[6] K. A. Schroder and K. W. Gentle, Phys. Plasmas **10**, 760 (2003).
[7] P. V. Savrukhin, Phys. Plasmas **9**, 3421 (2002).
[8] J. R. Martín-Solís, R. Sánchez, and B. Esposito, Phys. Plasmas **6**, 3925 (1999).
[9] A. V. Gurevich and K. P. Zybin, Phys. Usp. **44**, 1119 (2001).
[10] P. B. Parks, M. N. Rosenbluth, and S. V. Putvinski, Phys. Plasmas **6**, 2523 (1999).
[11] F. Andersson, P. Helander, and L.-G. Eriksson, Phys. Plasmas **8**, 5221 (2001).
[12] J. R. Martín-Solís, R. Sánchez, and B. Esposito, Phys. Plasmas **7**, 3814 (2000).
[13] J. R. Dwyer, Geophys. Res. Lett. **31**, L12102, (2004).
[14] B. Esposito, J. R. Martín-Solís, F. M. Poli, J. A. Mier, R. Sánchez, and L. Panaccione, Phys. Plasmas **10**, 2350 (2003).

[15] J. R. Martín-Solís, B. Esposito, R. Sánchez, and J. D. Alvarez, Phys. Plasmas **6**, 238 (1999).
[16] H. Smith, P. Helander, L.-G. Eriksson, D. Anderson, M. Lisak, and F. Andersson Phys. Plasmas **13**, 102502 (2006).
[17] J. R. Martín-Solís, R. Sánchez, and B. Esposito, Phys. Plasmas **7**, 3369 (2000).
[18] C. B. Moore, K. B. Eack, G. D. Aulich, and W. Rison, Geophys. Res. Lett. **28**, 2141 (2001).
[19] J. R. Dwyer, M. A. Uman, H. K. Rassoul, M. Al-Dayeh, E. L. Caraway, J. Jerauld, V. A. Rakov, D. M. Jordan, K. J. Rambo, V. Corbin, and B. Wright, Science **299**, 694 (2003).
[20] J. R. Dwyer, M. A. Uman, H. K. Rassoul, V. A. Rakov, M. Al-Dayeh, E. L. Caraway, B. Wright, J. Jerauld, D. M. Jordan, K. J. Rambo, A. Chrest, and C. Smyth, Geophys. Res. Lett. **31**, L05118 (2004).
[21] J. R. Dwyer, M. A. Uman, H. K. Rassoul, V. A. Rakov, M. Al-Dayeh, E. L. Caraway, B. Wright, J. Jerauld, D. M. Jordan, K. J. Rambo, A. Chrest, and C. Smyth, Geophys. Res. Lett. **31**, L05119 (2004).
[22] J. R. Dwyer, M. A. Uman, H. K. Rassoul, V. A. Rakov, M. Al-Dayeh, E. L. Caraway, B. Wright, J. Jerauld, D. M. Jordan, K. J. Rambo, A. Chrest, and E. Kozak, Geophys. Res. Lett. **32**, L01803 (2005).
[23] G. K. Parks, B. H. Mauk, R. Spiger, and J. Chin, Geophys. Res. Lett. **8**, 1176 (1981).
[24] K. B. Eack, W. H. Beasley, W. D. Rust, T. C. Marshall, and M. Stolzenburg, Geophys. Res. Lett. **23**, 2915 (1996).
[25] K. B. Eack, D. M. Suszcynsky, W. H. Beasley, R. Roussel-Dupre, and E. Symbalisty, Geophys. Res. Lett. **27**, 185 (2000).
[26] J. R. Dwyer, H. K. Rassoul, Z. Saleh, M. A. Uman, J. Jerauld, and J. A. Plumer, Geophys. Res. Lett. **32**, L20809 (2005).
[27] G. J. Fishman, P. N. Bhat, R. Mallozzi *et al.*, Science **264**, 1313 (1994).
[28] D. M. Smith, L. I. Lopez, R. P. Lin, and C. P. Barrington-Leigh, Science **307**, 1085 (2005).
[29] J. R. Dwyer and D. M. Smith, Geophys. Res. Lett. **32**, L22804 (2005).
[30] V. A. Rakov and M. A. Uman, *Lightning Physics and Effects* (Cambridge University Press, Cambridge, UK, 2003), p. 84.
[31] D. R. MacGorman and W. D. Rust, *The Electrical Nature of Storms* (Oxford University Press, New York, 1998), Chap. 8, pp. 86–88, 174, 181.
[32] R. Solomon, V. Schroeder, and M. B. Baker, Q. J. R. Meteorol. Soc. **127**, 2683 (2001).
[33] A. V. Gurevich, G. M. Milikh, and R. Roussel-Dupré, Phys. Lett. A **165**, 463 (1992).
[34] J. R. Dwyer, Geophys. Res. Lett. **30**, 2055 (2003).
[35] A. V. Gurevich, G. M. Milikh, and J. A. Valdivia, Phys. Lett. A **231**, 402 (1997).
[36] L. P. Babich, E. N. Donskoy, I. M. Kutsyk, and R. A. Roussel-Dupré, Geophys. Res. Lett. **32**, L09809 (2005).
[37] J. R. Dwyer, Geophys. Res. Lett. **32**, L20808 (2005).
[38] J. R. Dwyer, L. M. Coleman, R. Lopez, Z. Saleh, D. Concha, M. Brown, and H. K. Rassoul, Geophys. Res. Lett. **33**, L22813 (2006).
[39] H. Dreicer, Phys. Rev. **115**, 238 (1959).
[40] A. V. Gurevich, Sov. Phys. JETP **12**, 904 (1961).
[41] N. G. Lehtinen, T. F. Bell, and U. S. Inan, J. Geophys. Res. **104**, 24699 (1999).
[42] L. M. Coleman and J. R. Dwyer, Geophys. Res. Lett. **33**, L11810 (2006).
[43] V. B. Berestetskii, E. M. Lifshitz, and L. P. Pitaevskii, *Quantum Electrodynamics* (Pergamon Press, Oxford, 1982), pp. 321–324, 326, 330–336, 356, 368–370.
[44] J. J. Sakurai, *Advanced Quantum Mechanics* (Addison-Wesley, Redwood City, CA, 1967), pp. 193–194.
[45] N. F. Mott and H. S. W. Massey, *The Theory of Atomic Collisions*, 3rd ed. (Oxford University Press, London, 1965), pp. 460–464.
[46] H. W. Koch and J. W. Motz, Rev. Mod. Phys. **31**, 4920 (1950).
[47] M. J. Berger, J. H. Hubbell, S. M. Seltzer, J. Chang, J. S. Coursey, R. Sukumar, and D. S. Zucker, XCOM: Photon Cross Sections Database (http://physics.nist.gov/PhysRefData/Xcom/Text/XCOM.html).
[48] N. A. Dyson, *X-rays in Atomic and Nuclear Physics*, 2nd ed. (Cambridge University Press, Cambridge, UK, 1990), pp. 215–225.
[49] S. C. Brown, *Introduction to Electrical Discharges in Gases* (Wiley, New York, 1966), pp. 119–129, 188.
[50] S. J. Desch, W. J. Borucki, C. T. Russell, and A. Bar-Nun, Rep. Prog. Phys. **65**, 955 (2002).
[51] H. B. Niemann, S. K. Atreya, G. R. Carignan, *et al.*, J. Geophys. Res. **103**, 22831 (1998).
[52] J. M. Meek and J. D. Craggs, *Electrical Breakdown of Gases* (Oxford, UK, 1953), p. 177.
[53] A. M. Hillas, *Cosmic-Rays* (Pergamon, Oxford, 1972), p. 50.
[54] T. C. Marshall, M. Stolzenburg, C. R. Maggio, L. M. Coleman, P. R. Krehbiel, T. Hamlin, R. J. Thomas, and W. Rison, Geophys. Res. Lett. **32**, L03813 (2005).
[55] L. A. Capone, J. Dubach, R. C. Whitten, and S. S. Prasad, Icarus **39**, 433 (1979).
[56] A. V. Gurevich, K. P. Zybin, and R. A. Roussel-Dupré, Phys. Lett. A **254**, 79 (1999).
[57] D. A. Smith, X. M. Shao, D. N. Holden, C. T. Rhodes, M. Brook, P. R. Krehbiel, M. Stanley, W. Rison, and R. J. Thomas, J. Geophys. Res. **104**, 4189 (1999).
[58] A. V. Gurevich, L. M. Duncan, Yu. V. Medvedev, and K. P. Zybin, Phys. Lett. A **301**, 320 (2002).
[59] Y. Yair, Z. Levin, and S. Tzivion, Icarus **115**, 421 (1995).
[60] G. F. Knoll, *Radiation Detection and Measurement*, 3rd ed. (Wiley, New York, 2000), pp. 159–188.
[61] E. Nasser, *Fundamentals of Gaseous Ionization and Plasma Electronics* (Wiley, New York, 1971), pp. 219–220, 426–430.
[62] C. T. R. Wilson, Proc. Cambridge Philos. Soc. **22**, 534 (1925).